Classical trajectory study of internal energy distributions in unimolecular processes

J. D. McDonald and R. A. Marcus

Department of Chemistry, University of Illinois, Urbana, Illinois 61801 (Received 15 March 1976)

The method of classical trajectories has been used to study the flow of energy in a molecular system (similar to the molecules CD₂Cl and CD₂H) representing a chemical activation experiment. Energy distributions are obtained both before and after the breakup of the activated molecule by means of a correlation function technique. Four different potential energy surfaces are employed. It is found that the initial distribution of energy in the activated molecule may or may not be random, depending on the details of the particular surface. This distribution becomes random in less than 5×10^{-12} sec. The distribution of energy in the final product (CD₃) is found to be randomly distributed (as predicted by RRKM theory including angular momentum considerations) for a surface with no exit channel barrier or strong intermode couplings. When these special forces are present nonrandom energy distributions result. Product channel barriers result in an excess of translational energy and exit channel intermode couplings result in nonrandom vibrational distributions. Angular momentum considerations are found to be important in matching the predictions of RRKM theory with the calculations.

INTRODUCTION

In the past few years, molecular beam, ¹ infrared chemiluminescence, ² and laser fluorescence³ experiments, and classical trajectory calculations⁴ using digital computers have provided a clear description of the dynamical properties of simple three-body chemical reactions. The measurement of final state distributions of the products of reactions whose collisions require only a few vibrational periods provides a wealth of information which can clearly define the shape of the potential energy surface upon which the reaction occurs. It is clear from these experiments and calculations that no simple (e.g., statistical) theory can describe, in detail, all the data.

Until very recently statistical theories have been able to adequately describe complex reactions, those involving several atoms and activated molecules lasting hundreds of vibrational periods or longer. All the available data (consisting of rate constants) could be explained by some variant of statistical theory, usually RRKM⁵ theory. The central tenet of this theory is the assumption of a random distribution lifetimes of the activated molecule. The original RRKM theory itself does not predict product state distributions, although it can be made to do so if angular momentum is properly considered, ⁵ and another statistical model, phase space theory, ⁷ also does so. These two theories assume a random distribution of energy in the activated complex.

There are now several experiments which show deviations from statistical behavior, either of lifetimes or of product energy distributions. Classical chemical activation experiments have shown deviations from RRKM lifetime predictions, molecular beam experiments have shown product translational state distributions which differ from unadjusted phase space theory predictions, 20,10 and infrared chemiluminescence experiments 11 have shown deviations from phase space theory predictions of product internal state distributions. There

have also been several classical trajectory studies on complex systems. ¹²⁻¹⁶ However, all but one of these studies have concerned themselves with short-lived (<10⁻¹² sec) activated molecules, rather high energies, and have centered attention primarily upon lifetime distributions.

In this paper the central question of how the energy present in an activated molecule distributes itself, and how it is disposed of among the modes of the products, is addressed directly. We have used here an approach which is essentially in the spirit of the experiments. This approach involves calculating, averaged over a (small) interval of time, the classical vibrational spectrum of each (approximate) normal mode of the activated molecule or product. In order to simplify the calculations as much as possible we have chosen a system which has only one (entrance and exit) channel, that is, it models a chemical activation energy transfer experiment. We have performed calculations on four different potential surfaces, all roughly representing CD,X, where X is H or Cl. In the case of CD2Cl, the trajectories are started by adding Cl to CD3, while the CD3H trajectories were started as CD₃H with a pseudorandom internal energy distribution (in order to conserve computer time).

We have chosen four different potential energy surfaces, which are essentially identical at the equilibrium geometry of CD₂X and at X+CD₃, differing only in the neighborhood of the (single) activated complex. The calculations provide the distribution of lifetimes, the product translational, rotational, and vibrational energy distributions, and actually show the approach to equilibrium of an initially nonrandom CD₂Cl state distribution produced by the nonrandom initial conditions.

These calculations were not designed to provide a comprehensive diagnostic survey of the possible behavior of a group of systems, but only to provide an example of as many expected or suspected effects as possible, using a few sets of trajectories.

THE CALCULATIONS

The four model surfaces used in this study were

$$\begin{split} V &= 9 \left\{ R_{\text{LC}} - 1 - \delta_3 \, 0. \, 14 \exp[-7(R_{\text{XC}} - 2. \, 5)^2] \right\}^2 & \text{(LC stretch)} \\ &+ 9 \left\{ R_{\text{MC}} - 1 - \delta_3 \, 0. \, 14 \exp[-7(R_{\text{XC}} - 2. \, 5)^2] \right\}^2 & \text{(MC stretch)} \\ &+ 9 \left\{ R_{\text{HC}} - 1 - \delta_3 \, 0. \, 14 \exp[-7(R_{\text{XC}} - 2. \, 5)^2] \right\}^2 & \text{(NC stretch)} \\ &+ 1. \, 5 \left[(R_{\text{LM}} - 1. \, 67303)^2 + (R_{\text{LN}} - 1. \, 67303)^2 + (R_{\text{HM}} - 1. \, 67303)^2 \right] & \text{(LM, LN, NM stretches)} \\ &+ 1. \, 75 \left\{ 1 - \exp[3.4042(1.6 - R_{\text{XC}})] \right\}^2 & \text{(XC stretch)} \\ &+ \frac{15}{1 + 0.0009 R_{\text{XC}}^{12}} \left\{ \left[\frac{R_{\text{XL}}^2 - (R_{\text{LC}} - R_{\text{XC}})^2}{4R_{\text{LC}}R_{\text{XC}}} - 0. \, 62941 \right]^2 & \text{(XCL bend)} \\ &+ \left[\frac{R_{\text{XM}}^2 - (R_{\text{MC}} - R_{\text{XC}})^2}{4R_{\text{MC}}R_{\text{XC}}} - 0. \, 62941 \right]^2 \right\} & \text{(XCM bend)} \\ &+ \left[\frac{R_{\text{XN}}^2 - (R_{\text{NC}} - R_{\text{XC}})^2}{4R_{\text{NC}}R_{\text{XC}}} - 0. \, 62941 \right]^2 \right\} & \text{(XCN bend)} \\ &+ \delta_2 \, 0. \, 33 \exp[-7(R_{\text{XC}} - 2. \, 5)^2] & \text{(XC exit barrier)} \\ &+ \delta_4 \, 0. \, 25 \exp[-\frac{19}{2}(R_{\text{XL}} + R_{\text{XM}} + R_{\text{XN}} - 9. \, 9)^2] \, , & \text{(XLMN exit barrier)} \\ \end{split}$$

where X is the chlorine or hydrogen atom, C is the carbon, and L, M, and N are deuteriums; $R_{\rm XC}$ is the distance between X and C; and δ_2 , δ_3 , and δ_4 indicate terms present only in surfaces 2, 3, and 4, respectively. Energies are given in eV and distances in Å. The masses of H, D, C, and Cl were taken to be 0.959, 1.918, 11.506, and 33.56 AMU, giving a unit of time equivalent to 10^{-14} sec. Each of the four surfaces are essentially the same in regions describing either separated X and CD₃ particles, or a bound CD₃X molecule. They are specifically designed to be different only in the region of the activated complex.

Surface 1 has no barrier to the departure of the X atom. Surface 2 has a simple barrier in the X-C stretching coordinate at a C-X distance of 2.6 Å and an energy of 0.25 eV. Surface 4 has a barrier also, but in this case the forces act between the X atom and the

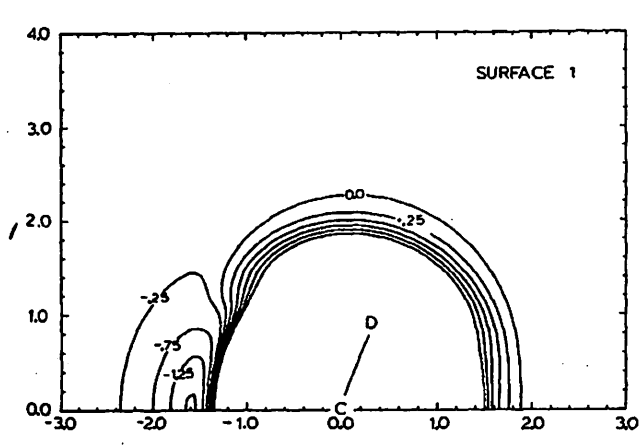


FIG. 1. Portion of surface 1, with CD_3 at its equilibrium distances, and X at a variable distance from CD_3 . The horizontal axis in this graph is the C_3 axis of CD_3 , and the vertical axis is the coordinate perpendicular to this axis. Distances are in units of 10^{-10} meter and energies in eV. The zero of energy refers to separated $X+CD_3$. Unlabeled contours are spaced at intervals of 0.5 eV. The atom approaches from the left in these trajectory studies.

three D atoms rather than between the X and C atoms as in surface 2. Surface 3 has a coupling between the C-X coordinate and the C-D coordinates such that the C-D bonds must be stretched to allow the X to leave without a large activation energy.

Graphs of a cross section of the entrance (and exit) channel of surfaces 1 and 2 are given in Figs. 1 and 2. Graphs such as these are really inadequate representations of these multidimensional surfaces, especially for surfaces 3 and 4, where several different bond coordinates are coupled together. Although this functional form for the potential contains several harmonic appearing terms, the nonorthogonality of the various coordinates results in the potential being highly anharmonic when expanded along zero-order normal coordinates. The shape of the inversion mode of CD₃ is similar to that of real NH₃; the equilibrium geometry of the

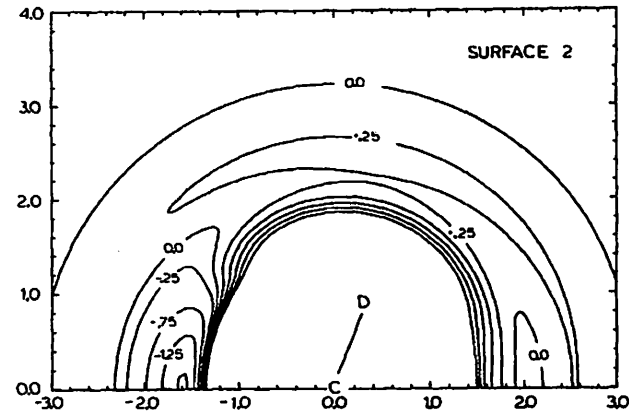


FIG. 2. Portion of surface 2, with CD₃ at its equilibrium distances, and X at a variable distance from CD₃. The horizontal axis is this graph is the C₃ axis of CD₃, and the vertical axis is the coordinate perpendicular to this axis. Distances are in units of 10^{-19} meter and energies in eV. The zero of energy refers to separated X+CD₃. Unlabeled contours are spaced at intervals of 0.5 eV. The atom approaches from the left in these trajectory studies.

TABLE I. Normal mode frequencies.

	Frequencies (cm ⁻¹)							
Mode	CD ₃	CD3H	CD3Cl	CD3Hp	CD ₃ Cl ^b			
1	1949	3530	1955	1949	1949			
2	1843ª	1948	1854ª	1843ª	1843ª			
3	602ª	1861ª	1361	602ª	602ª			
4	292	1339ª	961ª	319	319			
5		1097	798	132ª	113ª			
6		601ª	600ª					

^aDoubly degenerate.

bActivated complex for surface 1.

CD₃ group in this model is the same in both CD₃ and CD₃X. The barrier to CD₃ inversion (0.03 eV) is smaller than the average product excitation, and this potential appears basically as a harmonic potential with only a small area near the minimum appearing quartic. The resulting anharmonicity is small enough that at the average excitation in these calculations, the quartic terms are unimportant. The normal mode vibration frequencies obtained from this potential are given in Table I.

This potential is not a particularly good fit to the real CH_3Cl molecule, as it cannot, for instance, dissociate to CH_3Cl+H or CH_3+HCl . It is actually more like the real potential of CH_3I , which has a C-I dissociation energy closer to the value used in our potential. The vibrational frequencies of our model are in the same range as those of real CD_3Cl but are not in the correct order. The potential is best considered as being typical of this sized molecule and not as a model of real CD_3Cl (or CD_3H).

The CD₂Cl activated molecules were formed by the addition of Cl to CD. Because such a large amount of internal energy, 2.563 eV (1.75 eV from potential attraction of Cl and CD, and 0.813 eV from relative translation) is created by the addition of Cl to CD, (in our model) the effect of vibration and rotation in the incoming CD, has been neglected, and all trajectories in the Monte Carlo study were started with the CD₃ at rest, neither vibrating nor rotating. The initial angle of approach and impact parameter were selected randomly, except that approach was limited to the front side of the CD₃ (see Fig. 1) and the impact parameter limited to 2.2 Å. The actual trajectories were computed by integrating Hamilton's Eqs. (24 first order equations) in Cartesian coordinates, the center of mass being held fixed.

Attempts to start the CD₂H trajectories by this method were unsuccessful, since the high velocity of the incoming H atom causes almost all trajectories to represent simple (<10⁻¹³ sec long) encounters and not long-lived activated molecules. We therefore started the CD₂H trajectories with a pseudorandom distribution of energy in CD₂H vibrations. This was done by choosing the five particles to be initially at rest (hence with zero linear and angular momenta) with a random extension in each normal coordinate. The total amount of internal energy, 2.50 eV, was obtained by adjusting the total amount of displacement keeping the ratio of energy

among modes fixed. One batch of trajectories was run using this starting method, using X=Cl and surface 1, in order to test the effect of the zero total angular momentum condition. For this sampling method trajectories dissociating at times less than 1.5 ps for CD₃Cl or 0.5 ps for CD₃H were discarded, in order to sample only products from randomized trajectories.

The small number of trajectories in each batch is a consequence of the extreme complexity (and great length) of each trajectory and the need to minimize computer costs. The fastest vibrational period is $\frac{1}{110}$ ps, and since some trajectories were allowed to run for 32 ps, there were up to 4000 vibrational periods in a trajectory. Several integration routines were tried including 6th and 12th order Adams, 4th order RungeKutta, and 6th order hybrid Gear, 17 all being tried with both fixed and variable step size. In all cases the effects of using a variable step size were nil or even deleterious, as the error parameters used for step size testing seldom changed. The best method was the 6th order hybrid Gear method, using with a fixed step size of 10^{-16} sec. Individual trajectories (for graphs, etc.) were run on a 360-75 computer, with double precision (56 bit mantissa) arithmetic, and batches for statistics were run on the Illiac IV array processor (with a 48 bit mantissa). 18

Extensive back-integration and step-size changing tests were done to determine the accuracy of these long trajectories. Each trajectory can be broken into one part, at early times, representing vibration of a CD₂X activated molecule, with ~2.5 eV excitation, and another part, at later times, representing CD, with <0.8 eV internal excitation. The part representing CD₃ alone is numerically accurate over its entire length and can be back-integrated to several significant figures. The CD₂X part of a trajectory proved to return to its starting point to two significant figures after back integration over any randomly chosen 2 to 3 ps section for CD,Cl and over 1.0 and 1.5 ps for CD,H; over longer sections inherent numerical instability in the dynamical equations combine with truncation and roundoff errors to make back-integration inaccurate. Since analysis of the final results shows that the nonrandomness introduced by the initial conditions decays faster than 3 ps for CD₂Cl or 0.5 ps for CD₂H the numerical inaccuracy introduced by the integration procedure should not effect the product state distributions resulting from activated molecules with long lifetimes. (If a distribution is already random, errors introduced by numerical instabilities have no effect on it. This point has been noted before concerning calculations on assemblies of particles 19). The parts of the trajectory which have ceased to reflect the initial conditions due to numerical instability cannot, however, be used to test the random lifetime distribution hypothesis or the rate of approach to randomness. Back integration is a very strong constraint on the accuracy. Several trajectories were found in which a nonrandom energy distribution remained fixed long after back integration became impossible. In all cases energy and total angular momentum are conserved to 10 decimal places for CD,Cl and seven places for CD.H.

Because of the anharmonicities and couplings between normal modes, there is no unique method for determining the energy in each "normal mode." The following method was devised to provide information about the vibrational spectrum of each normal mode of CD₃. A similar method was employed for CD₃X.

- (1) At points spaced 5×10⁻¹⁵ sec apart the center of mass of CD, molecule was first moved to the origin and the velocity of the center of mass subtracted off; then it was rotated about its center of mass until $\sum_{i=1}^{12} q_i r_{ii} = 0$, where the $12q_i$ are the displacements of the x, y, and zcoordinates of the four atoms from their equilibrium position, and r_{ii} , j=x, y, or z are three 12-dimensional vectors representing infinitesimal rotations about the x, y, and z axes. The three components of angular momentum are obtained at this step. Next the momenta in Cartesian coordinate, p_i , i=1, 12, were converted to a mass weighted coordinate system p_i : $p_i' = p_i \sqrt{M_i}$, where M_i is the mass of the atom associated with the i coordinate. Finally the momenta in each of the 6 mass weighted normal momentum coordinates θ_i , i=1,6, were computed $\mathcal{O}_j = \sum_{i=1}^{12} p'_i X_{ji}$, where X_{ji} are unit 12dimensional vectors representing motion along each of the six small-displacement normal modes.
- (2) The autocorrelation function²⁰ for each of the six momenta is next found:

$$C_j(T_0, \Delta T) = \sum_{K=1}^{M} \varphi_j(T_0 + K\delta) \varphi_j(T_0 + K\delta + \Delta T) ,$$

where T_0 is the time at the start of the time interval of width $\Delta T_{\rm max} = N\delta$ covered by this average. The times T_0 and ΔT are in integer steps of $\delta = 5 \times 10^{-15}$ sec. The resolution is proportional to the number of points N in this function. The value of N was variously 50, 128, or 256, depending on the needed resolution and also programming considerations. M must be greater than N.

(3) In order to obtain spectral peaks with no negative side lobes, the correlation function was given trapezoidal apodization²⁰:

$$C'(T_0, \Delta T) = C(T_0, \Delta T)^*(\Delta T_{\text{max}} - \Delta T)/\Delta T_{\text{max}}$$
.

This procedure changes the apparent shape of an isolated, monochromatic line from $\sin\alpha(\nu-\nu_0)/(\nu-\nu_0)$ to $[\sin\alpha(\nu-\nu_0)/(\nu-\nu_0)]^2$, where ν_0 is the central frequency and α is a constant depending on N.

(4) The momentum vibration spectrum²⁰ $S(T_0, \nu)$ was computed by taking the Fourier transform of $C'(T_0, \Delta T)$. This spectrum is given pointwise, from 0 to 3333 cm⁻¹ [0 to 9.92 10^{19} Hz], in N equal steps. The 3530 cm⁻¹ mode of CD₂H appears in an "alias"²⁰ at 3136 cm⁻¹. The spectrum of a coordinate conjugate to a given momentum is $S_0(\nu) = S_p(\nu)/\nu^2$. This exact relation²⁰ is a direct consequence of the properties of correlation functions and Fourier transforms.

This procedure which produces a mechanical vibration spectrum in each normal coordinate has two important features. (The word "spectrum" does not here imply radiation but refers to intensity (amplitude squared) of mechanical motion at a given frequency.) First, for small amplitude vibrations there is only one peak in the spectrum of each normal mode, and the area under this peak is proportional to the energy in the mode. Second, one may calculate an infrared or Raman spectrum of the vibrating molecule by taking the properly weighted linear combination of normal modes before taking the correlation function. For high amplitude vibrations the effect of coupling between modes appears as a broadening of lines and the growing in of subsidiary peaks due to cross modulation and "beats," and the energy in a mode is no longer precisely defined. The effect of anharmonic force fields will show clearly in the spectrum. For example, the vibrational frequency of a quartic oscillator increases with excitation, and a peak is present at 3 (and 5, 7, ...) times the fundamental frequency.

Distribution and averages of energy in each mode and in rotation and translation are computed in the usual manner. ^{21,23} The relation between spectral intensity (peak area) and energy was obtained by requiring the total vibrational energy, obtained from the spectrum, added to the rotational and translational energy, to equal the total energy. The proportionality constant thus obtained varied by only 5% between individual trajectories.

The total number of trajectories in each batch was varied in order to balance the requirements of adequate sampling and minimum computer time. The standard deviation 22 of a particular average energy value x (for one mode) is given by (for N trajectories)

$$\sigma \cong \frac{1}{\sqrt{N-1}} \sqrt{\frac{1}{N}} \sum_{i=1,N} (x_i - \langle x \rangle)^2 \ .$$

This quantity decreases with increasing N; $\sigma \simeq \text{const}/\sqrt{N}$. For all the batches listed, N was increased (in multiples of 64) until it was clear whether a given batch was statistical in vibration (i.e., the average energy was equal in each vibrational mode, allowing a difference of $\pm 15\%$ for systematic error in the spectral analysis procedure) within a 95% confidence limit. The usual standard deviation for the quantities listed in the tables various from 0.002 to 0.005, except for batches with very few trajectories (such as surface 1 for CD₃Cl started with no angular momentum).

RESULTS

The behavior of two individual trajectories typical of CD₃Cl is shown in Figs. 3, 4, and 5. (These are on a variant of surface 1 with the potential constants 1.75 and 3.4042 replaced by 3.00 and 2.60, respectively. The normal mode frequencies are the same as those of surface 1.) The total energy is 4.1 eV (1.1 eV above dissociation). The figures show the spectrum of each normal mode averaged over a 2.5 ps interval. The first portion of each trajectory represents the CD₂Cl activated molecule itself. Note the large fluctuations in the energy in each mode versus time, the varying width and structure of peaks, and the existance of subsidiary peaks at frequencies of other normal modes. At these high excitations, energy flows freely between modes, on a time scale short compared to 2.5 ps. The subsidiary peaks are caused by the coupling between modes due to the very wide amplitude of vibrational mo-

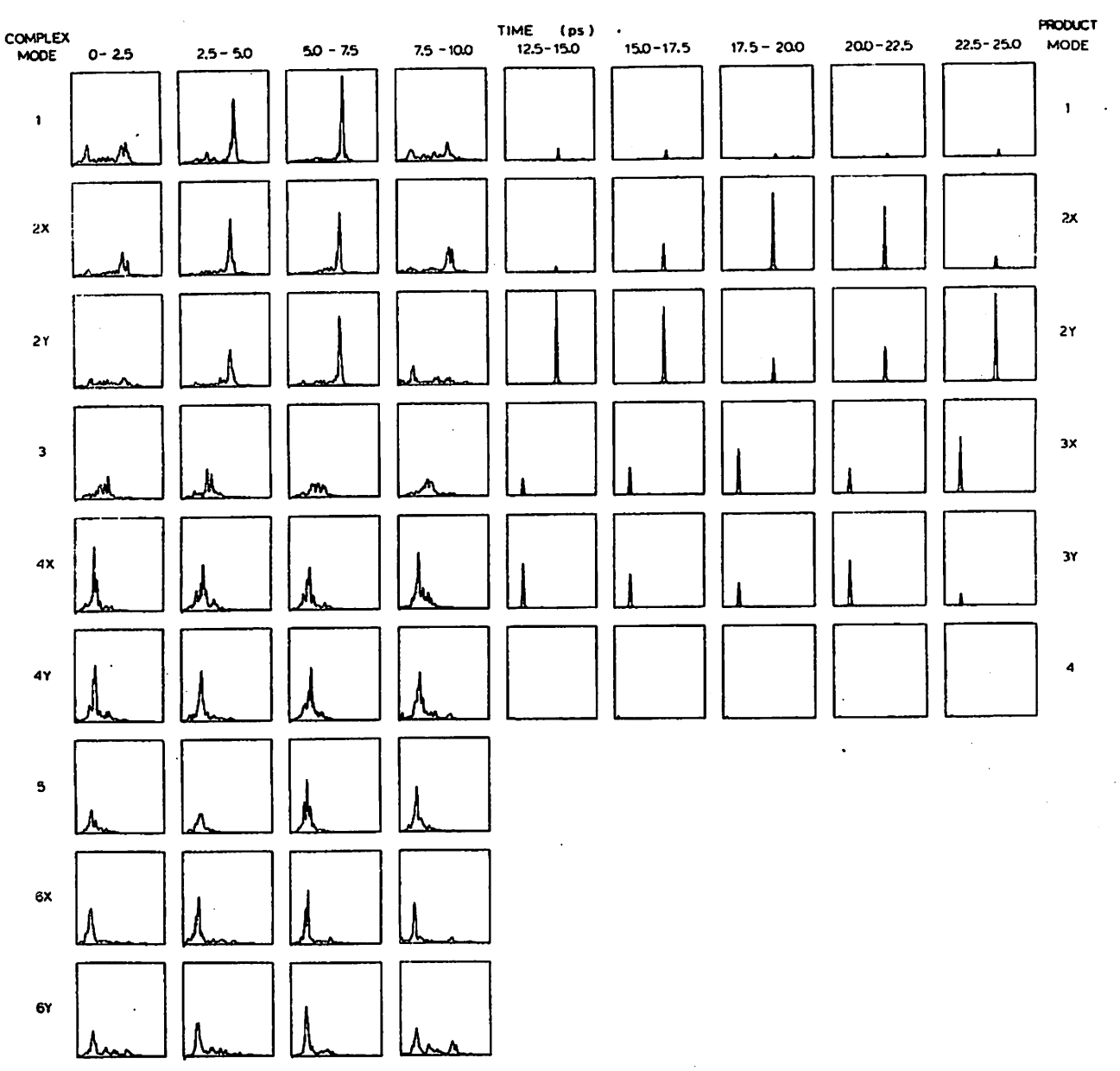


FIG. 3. Spectra of each normal coordinate vs. time for a single trajectory on a variant of surface 1, for CD₃Cl. Each individual frame gives the vibrational energy spectrum of a single mode averaged over a time of 2.5 ps. The horizontal axis is vibrational frequency (from 0 to 3333 cm⁻¹ in units of 13 cm⁻¹) and the vertical axes are energy/cm⁻¹. All the graphs have the same scale.

tion, far exceeding the region of good normal modes. Even at this very high energy, however, the vestiges of normal mode frequencies are clearly evident.

A perusal of similar plots shows that the presence of alternating plots with sharp peaks and plots with broad structure is typical, but that there is no pattern to the occurrence of these characteristics; they appear to be random in time.

The two trajectories vary most dramatically in the behavior of the product CD_3 molecule. In the trajectory of Fig. 3 the internal energy of the product CD_3 is 0.413 eV and the initial energy distribution is frozen over at least 12.5 ps. The energy in the nondegenerate modes (1 and 4) is essentially constant, while in the degenerate modes 2 and 3 only the total in the X and Y directions is constant. In the trajectory of Fig. 4, in

which the CD₃ group has an internal energy of 1.03 eV, the energy first appears mainly in mode 1 but later becomes more widely distributed. This process requires about 10 ps to occur; frames at times out to 40 ps show behavior similar to the last two shown.

Figure 4 shows a feature common to all trajectories at similar energies (both in CD₃ and CD₃X). At a time immediately before the energy appears to redistribute (at 15–17.5 ps in Fig. 2) one of the lesser active modes (mode 4 here) shows a peak not at its own frequency, but at a frequency of the *most* active mode. About 1 ps later this mode (No. 4 here) shows a strong activity at its normal frequency. Examination of the numerical values of the peak at the frequency of mode 1 in mode 4 shows that exponential growth in a very weakly energized mode is a very characteristic feature of all trajectories at medium (~1 eV) energies.

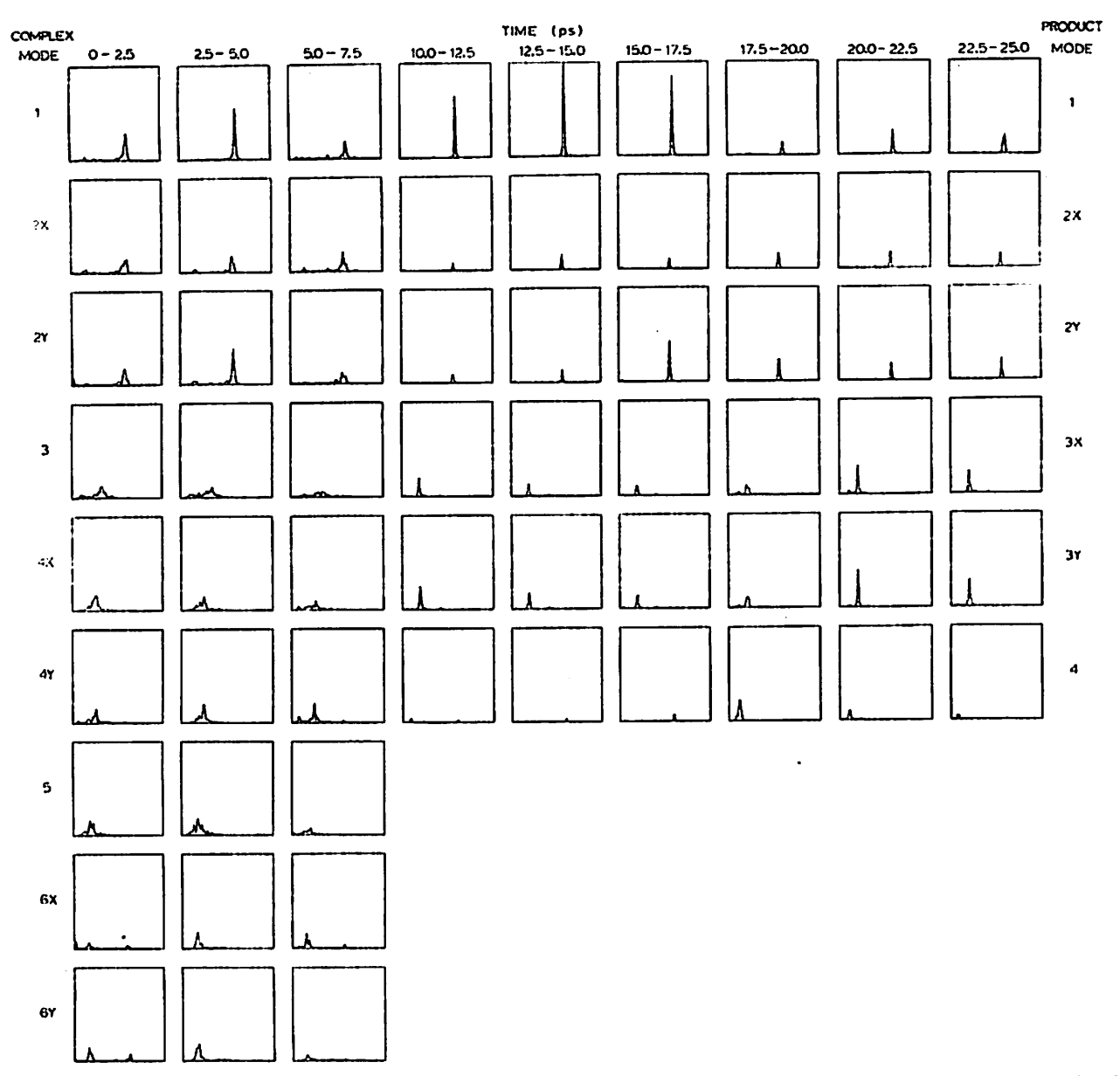


FIG. 4. Spectra of each normal coordinate vs. time for a single trajectory on a variant of surface 1, for CD₃Cl. Each individual frame gives the vibrational energy spectrum of a single mode averaged over a time of 2.5 ps. The horizontal axis is vibrational frequency (from 0 to 3333 cm⁻¹ in units of 13 cm⁻¹) and the vertical axes are energy/cm⁻¹. All the graphs have the same scale.

A portion of the actual normal mode oscillations of the trajectory in Fig. 4 is shown in Fig. 5. The variation of energy in each mode with time and the general tendency to vibrate at the frequency, bound in the ordinary normal mode analysis at least over short periods of time, are clearly evident.

The production of the CD₃Cl activated molecule by combination of two particles is clearly a nonrandom process, and should produce a nonrandom excitation of the CD₃Cl. Surfaces 1 and 3 were examined in detail to test for this effect. Figure 6 shows the time dependence of the energy in each normal mode for a set of 80 trajectories on surface 3 with total energy 1.90 eV. None of these trajectories dissociated in 2 ps. The average is given for the degenerate modes. The energy in the modes having the same symmetry as the reaction coordinate is higher than average, and decreases with

time, while in those with symmetry different from the reaction coordinate (the degenerate modes) it is low and increases. At long times the energy in each mode reaches a constant value equal within the systematic analysis error of about 10%. In addition, at long times (>3 ps) the spectrum of a long stretch of a single trajectory (say 30 ps) is independent of the starting conditions and is the same as the spectrum of an average 30 trajectories over 1 ps each. A similar analysis on surface 1 showed no perceptible variation of the distribution of energy versus time; the distribution begins in the same energy distribution as reached at long times on surface 3. Surfaces 2 and 4 were not tested for this effect.

Figure 7 shows the shape of the peaks for each normal mode, for an average of 80 trajectories on surface 3, for CD₃Cl, at times between 3.0 and 3.5 ps. The to-

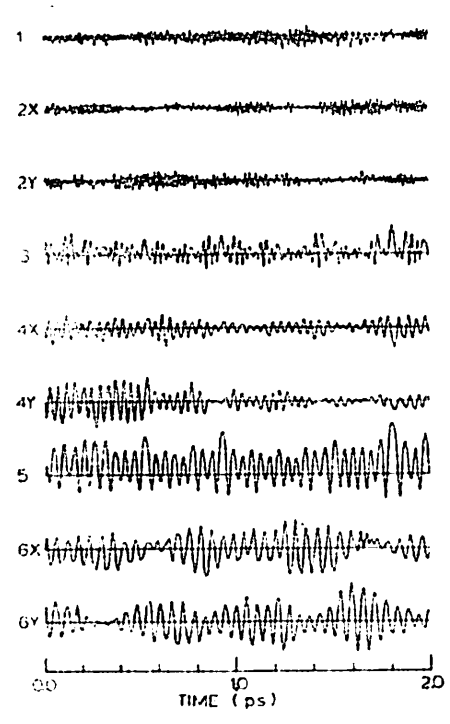


FIG. 5. Normal displacement coordinates vs. time (in mass. weighted coordinate systems) for a portion of the trajectory of Fig. 4. The portion covered here spans 3.0 to 5.0 ps in Fig. 4.

tal energy was 1.90 eV. The shape of these peaks is the same for a long stretch (>30 ps) of a single trajectory as for this multiple trajectory average.

The lifetime distributions for CD₃Cl on surfaces 1 (Fig. 8) and 3 show a clear nonexponential behavior. (Note that surface 1 shows no initial nonrandom energy distribution large enough to be statistically significant.) The original decay rate is faster than the long term rate, and the break between the two rates occurs at about 1.5 ps, about the same time that the nonrandom energy distribution disappears, but considerably earlier than the point at which the trajectories cease to be backintegratable. Although trajectories longer than 3 ps

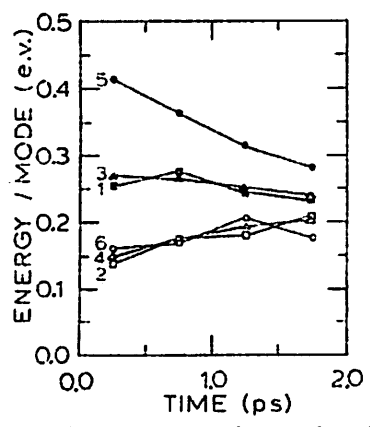


FIG. 6. Energy in each normal mode of the activated molecule vs. time, for an average of 80 trajectories on surface 3, for CD₃CI, started as Cl+CD₃, with 1.90 eV total energy. The average value is given for the degenerate modes. The numbers to the left of each curve are the mode indices (of Table I).

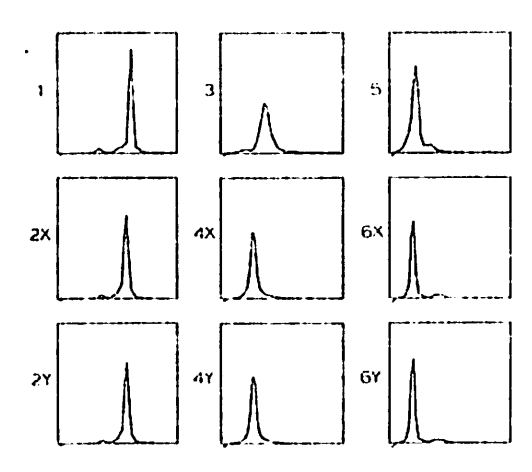


FIG. 7. Spectra of each normal mode, averaged over 80 trajectories of $Cl + CD_3$ on surface 3 at times between 3.0 and 3.5 ps. Horizontal axis is wavenumber between 0 and 3333 in steps of 67 cm⁻¹. Vertical axes are energy/cm⁻¹ on the same relative scale.

cannot be used to verify the random lifetime distribution assumption of RRKM theory, these longer trajectories do have the same lifetime distribution as those lasting 1.5 to 3 ps, which are back integrable, we believe that they can be used to establish the state distributions of product molecules, and also to test the predictions of RRKM theory for the rate of decay of already random activated molecules [that is, the predictions of Eq. (1)]. (Surfaces 2 and 4 do not have sufficiently many trajectories which break up at short times to allow analysis.)

The process used to start the CD_3H trajectories is also nonrandom, although in a more subtle manner. The distribution of energies is close to random, differing from a random one only because of the coupling of normal modes. However, the *phase* is clearly nonrandom as each trajectory was started with the atoms at rest. Tests similar to those used for CD_3Cl show that any nonrandom behavior is gone after 0.5 ps. Trajectories which dissociated before 0.5 ps were discarded.

The main results of this study consist of the energy distribution between the four vibrational modes, translation, and rotation in the product molecules. This data is given in Tables II and III. Because of the limited number of trajectories in each batch there is an appre-

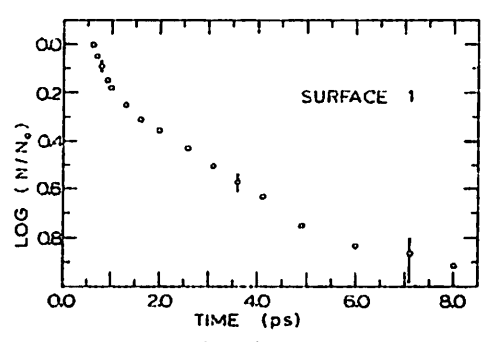


FIG. 8. Lifetime distribution for trajectories of CD₃Cl on surface 1, started as Cl + CD₃. N_0 is the number of complexes remaining undissoicated at t=0.6 ps.

TABLE II. Average energies in each product mode for trajectories started as Cl + CD₃. Values for modes 2 and 3 are the average of the two degenerate modes.

			Average energies (eV)						
	Time (10 ⁻¹² s)	Number of trajectories	1	2	3	4	Trans	Rot	
Surface	0.0-0.5	161	0.041	0.024	0.039	0.073	0.507	0,076	
1	0.5-1.5	170	0.089	0.078	0.079	0.096	0.225	0.102	
X C1	1.5-8.0	135	0.080	0.081	0.068	0.076	0.243	0.100	
	0.5-8.0 >8.0	305 46	0.085	0.080	0.074	0.087	0.233	0.101	
Surface	0.0-0.5	96	0.006	0.005	0.006	0.022	0.754	0.022	
3	0.5-32.0	75	0.068	0.064	0.057	0.058	0.398	9.081	
X = CI	>32.0	213					***************************************	3.002	
Surface	0.0-0.5	212	0.032	0.017	0.033	0.144	0.496	0.061	
3	0.5-1.5	180	0.062	0.058	0.069	0.107	0.266	0.120	
X = Cl	1.5-8.0	94 '	0.082	0.089	0.075	0.083	0.185	0.120	
	0.5-8.0	274	0.069	0.069	0.071	0.099	0.238	0.120	
	>8.0	26					0,120	0.200	
Surface	0.0-0.5	68	0.020	0.009	. 0.024	0.053	0.634	0.046	
4	0.5-16.0	150	0.051	0.053	0.053	0.083	0.400	0.070	
X== C1	>16.0	230				2,300			

ciable random error in the average values tabulated. Even for batches which are completely statistical in vibration (i.e., have the same average energy in each mode) there will be a statistical fluctuation and some spread is expected. We have decided between random deviations and true nonrandom behavior with the following method: if the most populated mode is greater than 1.3 times the least populated (in vibration), then the deviation is considered nonrandom. This assures that there will be less than a 1% chance that a random distribution will be labeled nonrandom due to statistical fluctuations.

By this criterion all four surfaces used for CD₃Cl show nonrandom behavior for trajectories whose collision lifetimes are shorter than 0.5 ps. This behavior

is clearly a consequence of the fact that some trajectories never form complexes, and most of their energy remain in translation.

For CD_3Cl the only long-lived (> 0.5 ps) complexes which display nonrandom vibration are those on surface 4 (at all times > 0.5 ps) and those on surface 3 which lasted greater than 0.5 but less than 1.5 ps.

All CD_3H trajectory sets were statistical in vibration except those on surface 3, which showed nonrandom behavior at all times greater than 0.5 ps.

The distribution of energy in a single mode versus the energy in that mode given by these calculations is given in Figs. 9-11.

TABLE III. Average energies in each product mode for trajectories started as CD_3X with no angular momentum. Values for modes 2 and 3 are the average of the two degenerate modes.

					Average Energies (eV)			
	Time (10 ⁻¹² s)	Number of trajectories	1	2	3	4	Trans	Rot
Surface	0.5-1.5	232	0.109	0.110	0.090	0.094	0.082	0.049
1	1.5-8.0	196	0.097	0.104	0.094	0.089	0.088	0.056
X=H	0.5—8.0 >8.0	428 71 .	0.104	0.107	0.092	0.092	0.085	0.052
Surface 2 X=H	0.5-10.0 >10.0	210 195	0.070	0.064	0.065	0.064	0.321	0.033
Surface 3 X=H	0.5—8.0 >8.0	237 66	0.076	0.099	0.090	0.109	0.192	0.068
Surface 1 X=Cl	1.5-8.0	93	0.098	0.065	0.098	0.073	0.088	0.093

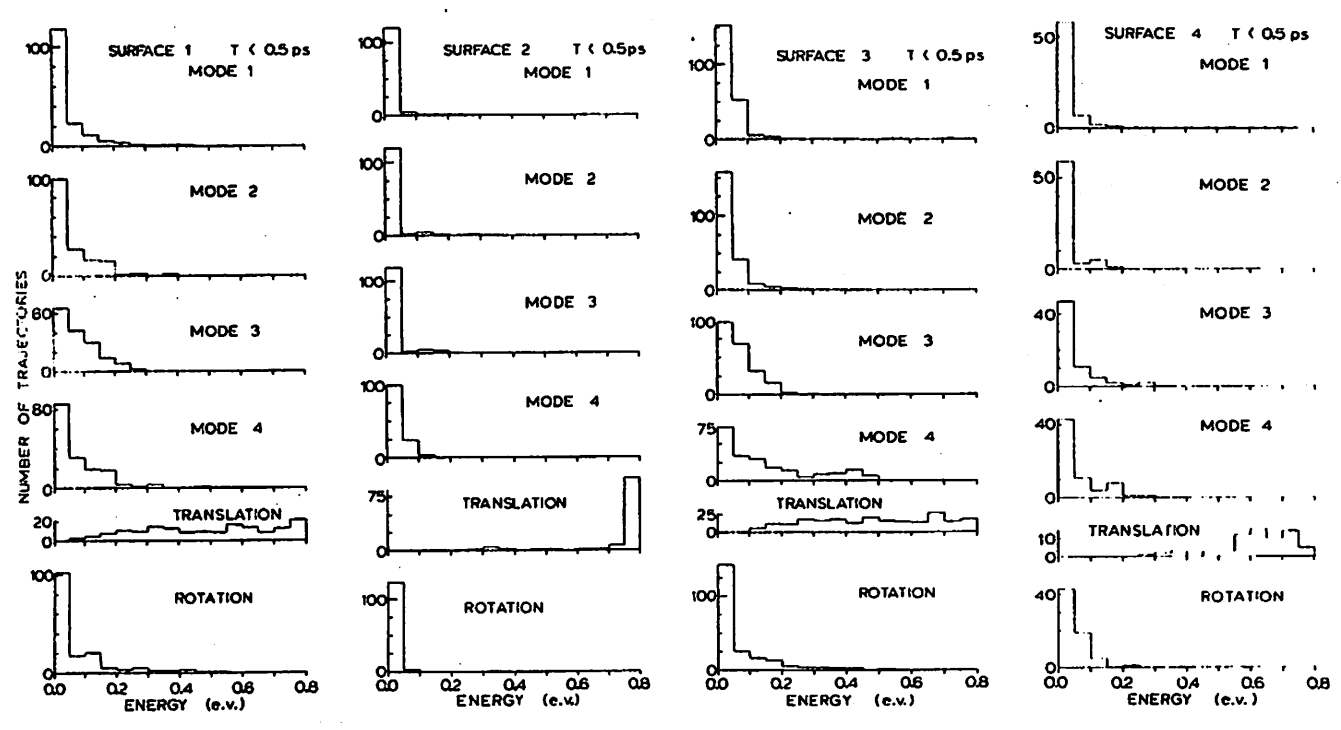


FIG. 9. Energy distributions for products from Cl+CD, for short-lived trajectories.

The distribution of energy in the nondegenerate vibrational modes is a decreasing (roughly exponential) function, while the distribution in the two doubly degenerate is peaked, as would be expected from the convolution of two (coupled) exponentially falling distributions. The rotational distributions are in all cases falling distributions.

The translational distributions show three different forms: In the two surfaces with product barriers (2 and

4) the effect of these barriers is dominant and produces a peaked distribution which is zero at low energies, and begins rising somewhat below the actual barrier height. The width of this distribution is greater in the CD₃Cl case (due to the increased total angular momentum).

On the surfaces without exit channel barriers (1 and 3) the presence or absence of total angular momentum makes a dramatic effect on the translational energy distribution. Where there is zero total angular momentum,

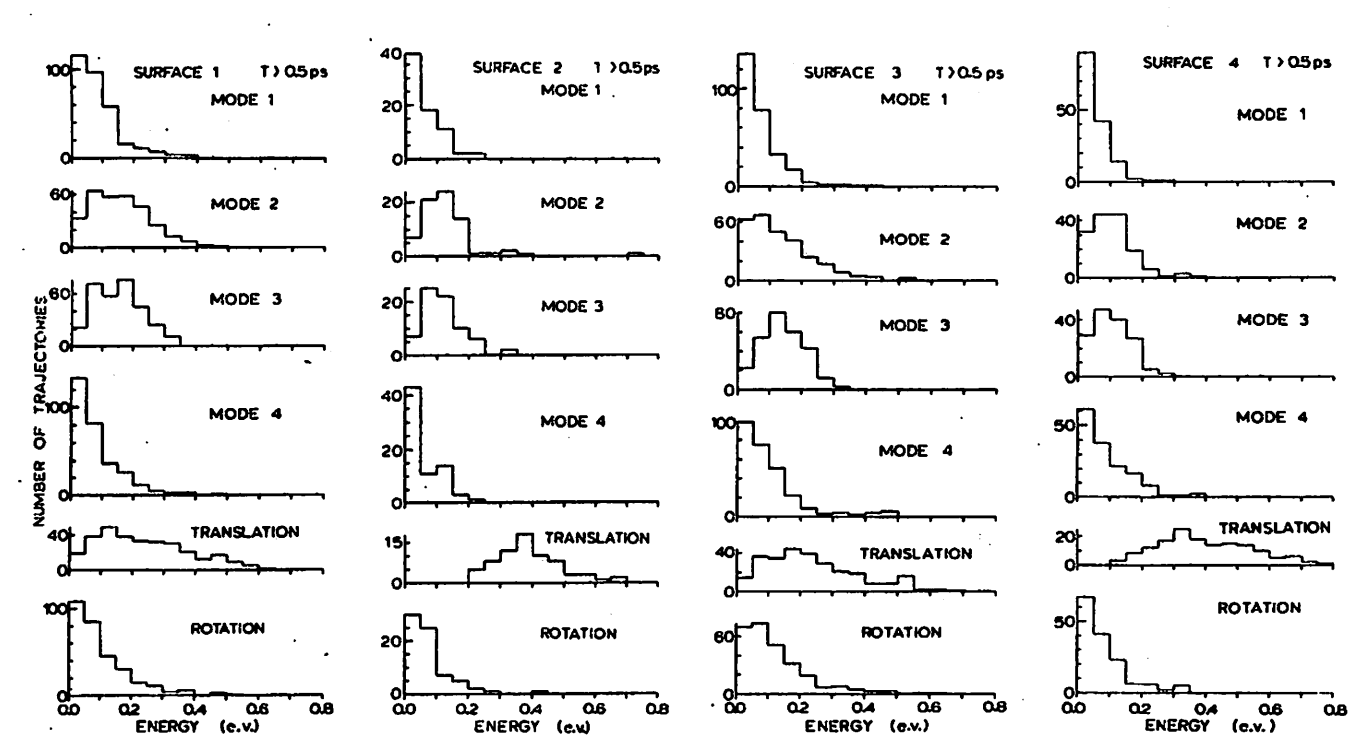


FIG. 10. Energy distribution for products from Cl+CD3 for long-lived trajectories.

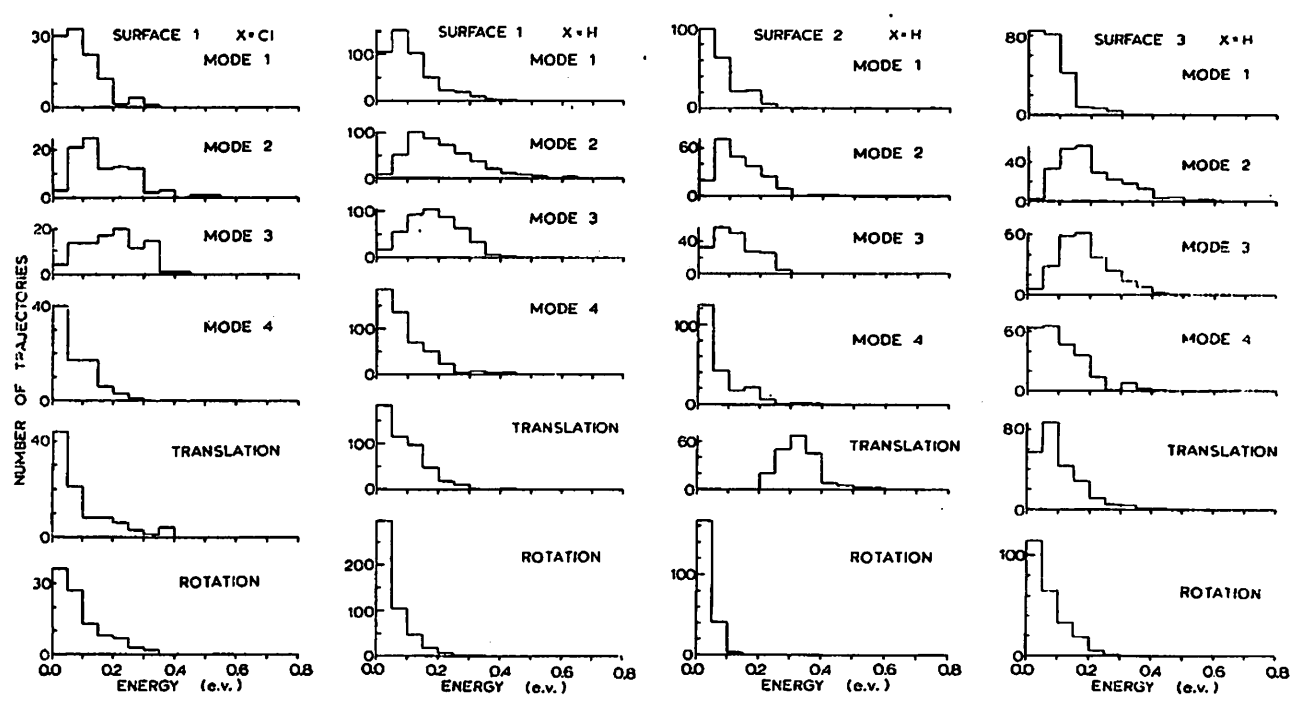


FIG. 11. Energy distribution for products started as CD₃X with no angular momentum.

the distribution is a monotone decreasing function of energy while with nonzero angular momentum it is a peaked function.

The effect of the total angular momentum on the translational and rotational energies is clearly evident in these figures. The trajectories which were started by adding a Cl atom to CD_3 (and thus have average total angular momentum of 18 \hbar) have *much* higher product translational energy and somewhat higher rotational energy than those started with no angular momentum (for either X = H or Cl).

We have also searched through the results of C1+CD₃ on surface 1 for correlations between two significant random initial conditions, impact parameter and the initial angle between the relative velocity vector and the C₃ axis of CD₃, and the final conditions. There is a reduced probability of forming a long-lived (>0.5 ps) complex at high impact parameters, and also for atoms hitting CD₃ nearly perpendicular to the C₃ axis. The most dramatic correlation is between the impact parameter and the final translational energy (Fig. 12). Clearly the total angular momentum (proportional to impact parameter, because there is no initial molecular rotation), which is conserved throughout a collision, very strongly controls the final translational energy.

DISCUSSION

Results of trajectory calculations such as these can be looked upon either as "calculations" with which real experiments can be compared, or as "experiments" which serve to verify the predictions of some (hopefully simpler) theory. The obvious comparison of the second sort is to RRKM or phase space theory, while the lack of an exact fit to "real" CD₃X renders the first sort of comparison inappropriate. We shall first compare our

calculations to statistical theories of the simplest sort and then point out the parts of our results which appear to be essentially dynamical, and hence outside the competence of any statistical theory. One of the basic assumptions of the theory of unimolecular reactions is that both the activated molecule and activated complex exist with a random distribution of states. The tests we have performed on the activated molecule tend to confirm the idea that, for complicated molecules and high enough energies (>2 eV), even if a molecule is formed with some special energy distribution, a random distribution will soon (<5 ps) be established by intramolecular relaxation. It is possible that effects which we have not tested for, such as nonrandom phase distributions or couplings between two mode's energies in a single trajectory (for example, modes 1 and 4 might

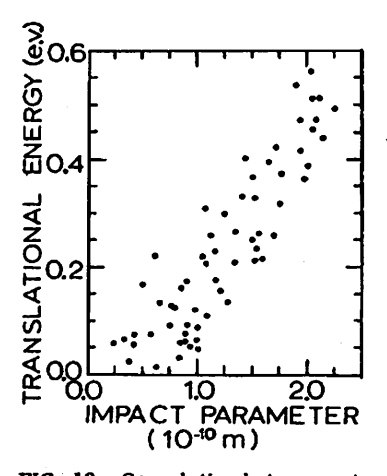


FIG. 12. Correlation between entrance channel impact parameter and final translational energy for activated molecules living longer than 0.5 ps on surface 1 for Cl+CD₃.

TABLE IV. Lifetimes for CD₂Cl started as Cl+CD₂ and CD₂H started with no angular momentum, with corresponding classical RRKM theory predictions.

	Lifetime (ps)				
	RRKM	Trajectory			
CD ₃ Cl					
Surtace 1	4.5	4.8			
Surface 2	180	105			
CD ₃ H					
Surface 1	1.0	4.9			
Surface 2	3.5	12			

always be highly or weakly excited together, but on the average be normally excited) might dilute this conclusion. This effect may indeed be present at short times on surface 1 for CD₅Cl, where tests show a random overall energy distribution but a nonexponential lifetime distribution. These trajectories also show that molecules which "react" before equilibrium is established will show the effects of the initial conditions on the final product states. A similar effect would be expected in a truly reactive case.

The results of this trajectory study are also in accord with recent findings of classical ergodic theory. ²³ For both CD₃Cl and CD₃ molecules, trajectories at low energies, less than about 1 eV total energy, show evidence of being in the quasiperiodic region (no energy mixing, sharp vibration frequencies, neighboring trajectories which separately approximately linearly with time)²⁴ while at higher energies they display ergodic behavior (random energy distributions, unsharp frequency of vibration, and exponentially separating trajectories).

The simplest comparison with statistical theory is a test of (fully classical) RRKM theory prediction of lifetimes. We have done this for surfaces 1 and 2 and for both CD₃H and CD₃Cl. According to the simplest application of RRKM theory, assuming all vibrations and two rotations active, and neglecting overall rotation.

$$\tau = \frac{1}{c} \frac{\prod_{i=1}^{6} \nu_{i}^{\dagger}}{\prod_{i=1}^{6} \nu_{i}} \left[\frac{E_{\text{tot}}(\text{activated molecule})}{\langle E_{\text{int}}(\text{activated complex})} \right]^{9} , \qquad (1)$$

the ν_i 's and ν_i^{\dagger} 's being the vibrational frequencies (in cm⁻¹) of the activated molecule and activated complex, respectively, and c the speed of light. The frequencies for the activated complex (Table I) were obtained at the C-X distance which yielded the longest lifetime (2.6 Å for surface 1 and 2.2 Å for surface 2). The results are given in Table IV, compared to the values obtained from the trajectory study by measuring the slope of $\ln(N/N_0)$ at times greater than 1.5 ps. We again emphasize that the use of trajectories which last longer than the accurate integration time is allowed here, as what Eq. (1) is designed to predict is the fraction of a group of activated molecules which will break up in some increment of time. It is possible to conceive of a group of molecules

• which have random lifetimes, but do not follow this formula (because, to cite one obvious example, some molecules which have crossed whatever surface is chosen as the critical configuration might return to form a new activated molecule). The trajectory and RRKM results are in fair agreement both for the cases illustrated and for surfaces 3 and 4 where the reaction coordinate is harder to define.

We have compared our product energy distributions and average energies (for surfaces 1 and 2) with statistical predictions. We have used a form of transition state theory (RRKM theory+angular momentum)²⁵ which includes the following features:

- (1) The transition state is located at a fixed location.
- (2) The transition state is considered "tight," although this makes little difference for the high angular momentum collisions.
- (3) The energy released when the outgoing particles descend the exit channel barrier on surface 2 all goes into translation.
- (4) The effect of the high total angular momentum present in the systems started as Cl + CD₃ is taken into account
 - (5) Classical distribution functions are used.

Item 4 is particularly important, as much of the translational energy of the products from Cl+CD₃ arises when the rotational motion of the complex is converted into translation as system descends the product (potential+centrifugal) barrier. For high angular momentum collisions the physical picture of the complex's dissociation is equivalent to the breaking of a dumbell-shaped molecule, with the particles leaving, on the average, tangentially.

Calculations using this model agree with both the average values and the distributions within the inherent accuracy expected from a simple model. In particular, the model predicts:

- (1) Equal amounts of energy in each vibrational mode.
- (2) The correct shape of the vibrational distribution:

$$P(\epsilon) = \text{const} (E_{\text{tot}} - E_{\text{barrier}} - \epsilon)^7$$

for single modes and

$$P(\epsilon) = \text{const } \epsilon (E_{\text{tot}} - E_{\text{barrier}} - \epsilon)^6$$

for the sum of the energy in a degenerate pair, in agreement with the trajectories.

(3) The qualitative differences in shape of the rotational and vibrational distributions for chlorine and hydrogen, and for sets with zero or nonzero angular momentum

The average values of energy in product translation and rotation for $Cl + CD_3$ are very dependent on the exact total angular momentum distribution and are fitted well ($\pm 25\%$) but not perfectly.

This model using semiclassical state counts²⁸ also gives reasonable agreement with the translational dis-

tributions measured by molecular beams for all the reactions

X + RCH = CHY - Y + RCH = CHX,

where X and Y are F, Cl, or Br, which last longer than one rotational period of the complex, but not for Y=H which probably needs exact quantum state counting.

The "special" effects which must be explained include the following:

- (1) The nonrandom lifetime distribution calculated for CD₃Cl on surfaces 1 and 3.
- (2) The nonrandom vibrational distribution observed on surfaces 3 and 4, even for activated molecules with a random energy distribution.
- '(3) The difference in vibrational distribution with time for CD₃Cl on surface 3.

The non-random lifetime distributions are clearly a consequence of the nonrandom initial conditions, and as mentioned previously it is possible to have a random energy distribution in the activated molecule (averaged over all trajectories) and still have a nonrandom lifetime distribution.

The nonrandom product vibrational distributions produced by trajectories which break up at long times (long enough to allow internal equilibration in the activated molecule) on surface 3 (for CD₃H) and surface 4 (for CD₂Cl) are a consequence of the special forces present in the exit channel. That surface 3 produces a nonrandom vibrational distribution on CD₂H only (for long times) may be a consequence of a "frequency" mismatch for CD₂Cl. The motion of the leaving Cl atom is so slow that the vibrational motions are essentially adiabatic. For the H which departs CD, H on surface 3. the speed is greater and there would be a better overlap of Fourier components of translation and vibration. Surface 4 does show a nonrandom effect on CD₃Cl because although the random distribution in the complex persists until the top of the barrier is reached, when the Cl descends the barrier it does so quickly, and the push against the three D atoms occurs quickly enough that they are excited. During this push the inertia of the C atom prevents it from following the motion of the D atoms.

Finally, the time dependence of the vibrational distribution on surface 3 (CD₃Cl) is probably due to the same decay vs time of the initial nonrandom energy distribution as was exhibited in Fig. 6. There are not enough short-lived (but snarled) trajectories on surface 4 for it to be analyzed for this effect.

Although the nonrandom effects shown here are not as dramatic as in direct three-body reactions (because most of the energy is above any possible barriers and couplings, and hence appears statistically distributed) they are equally indicative of the form of potential surface on which a reaction operates, and we believe that trajectory calculations can be as useful in analyzing complex trajectories as for simple ones. The problem is the incredible amount of computer time which must

be used to get results, and further such projects will need a large new infusion of funds.

ACKNOWLEDGMENTS

This work was supported by the National Science Foundation (Grant No. NPS 74-23140) and the National Aseronautics and Space Administration (Grant No. NGR 14-005-202).

We wish to thank Professor Bob Ray for the use of his access to the Illiac IV computer, and also to thank Dr. Don Noid for many helpful discussions especially concerning the relation of this work to classical ergodic theory.

Send reprint requests to JDM.

- R. Herschbach, Chem. Soc. Faraday Disc. 55, 233 (1973).
 A. M. G. Ding, L. J. Kirsch, D. S. Perry, J. C. Polanyi and J. L. Schreiber, Chem. Soc. Faraday Disc. 55, 252 (1973) and references cited therein.
- ³H. W. Cruse, P. J. Dagdigian and R. N. Zare, Chem. ::oc. Faraday Disc. 55, 277 (1973).
- ⁴J. C. Polanyi, Chem. Soc. Faraday Disc. 55, 389 (1973).
 ⁵P. J. Robinson and K. A. Holbrook, Unimolecular Reactions (Wiley, New York, 1972).
- ⁶R. A. Marcus, J. Chem. Phys. 62, 1372 (1975).
- C. Light, Disc, Faraday Soc. 44, 14 (1967); see also R.
 A. Marcus, Chem. Soc. Faraday Disc. 55, 379 and 381 (1973).
- ⁸J. D. Rynbrandt and B. S. Rabinovitch, J., Phys. Chem. 75, 2164 (1971). J. F. Meagher, K. J. Chao, J. R. Barker and B. S. Rabinovitch, J. Phys. Chem. 78, 2535 (1974).
- ⁹J. M. Parson and Y. T. Lee, J. Chem. Phys. 56, 4658 (1972); J. M. Parson, K. Shobatake, Y. T. Lee, and S. A. Rice, J. Chem. Phys. 59, 1402 (1973); K. Shobatake, J. M. Parson, Y. T. Lee, and S. A. Rice, J. Chem. Phys. 59, 1416 (1973); K. Shobatake, J. M. Parson, Y. T. Lee, and S. A. Rice, J. Chem. Phys. 59, 1427 (1973); K. Shobatake, Y. T. Lee, and S. A. Rice, J. Chem. Phys. 59, 1435 (1973); K. Shobatake, Y. T. Lee, and S. A. Rice, J. Chem. Phys. 59, 6104 (1973).
- ¹⁹J. T. Cheung, J. D. McDonald, and R. R. Herschbach, J. Amer. Chem. Soc. 95, 7889 (1973).
- ¹¹J. G. Moehlmann, J. T. Gleaves, J. W. Hudgens, and J. D. McDonald, J. Chem. Phys. **60**, 4790 (1974); J. G. Moehlmann and J. D. McDonald, J. Chem. Phys. **62**, 3052 (1975); J. F. Durana and J. D. McDonald, J. Chem. Phys. **64**, 2518 (1976).
- ¹²D. L. Bunker, J. Chem. Phys. 37, 393 (1962).
- ¹³D. L. Bunker, J. Chem. Phys. 40, 1946 (1964).
- ^MD. L. Bunker and W. O. Hase, J. Chem. Phys. **59**, 4621 (1973).
- ¹⁵W. L. Hase and D. F. Feng, J. Chem. Phys. 61, 4690 (1974). ¹⁸P. Brumer and M. Karplus, Chem. Soc. Faraday Disc. 56, co. (1972).
- ¹⁷Programmed by P. Brumer, Ref. 16, and P. Brumer, Ph.D. thesis, Harvard University, 1972.
- ¹⁸Each of these computers required 2 min to calculate 1 picosecond of trajectory. Thus the 360-75 required 1 h for a single 32 ps trajectory. The Illiac IV is an 64-wide array processor, that is, it processes 64 trajectories, each having the same differential equation but differing initial conditions, simultaneously. It processes 64 trajectories, each lasting 32 ps, in 1 h. Programs were coded in Fortran H on the 360-75 and in assembly language and Glypnir (an Algol-like language) on the Illiac IV.
- ¹⁸A. Rahman (private communication).
- ²⁰D. C. Champeney, "Fourier Transforms and their Physical

Applications" in Techniques of Physics, edited by G. K. T. Conn and K. R. Coleman (Academic, London, 1973), Vol. I. 21 The angular distributions were not calculated, as the restric-

tions on input impact parameter and angles would render them

22D. L. Bunker in Methods in Computational Physics, edited by A. Alder, S. Fernbach, and M. Rotenberg (Academic, New York, 1971).

²³J. Ford, Adv. Chem. Phys. 24, 155 (1973).

²⁴Special pairs of trajectories, with identical energy but initial

conditions differing by 10⁻⁵ Å in the 12-dimensional coordinate space were calculated for this purpose. Two pairs, for CD3Cl at 1.00 eV total energy, were run in quadruple precision (112 bit mantissa) with step size 0.0025×10-14 sec in order to avoid the numerical instability problem.

²⁵J. D. McDonald (to be published).

25G. Z. Whitten and B. S. Rabinovitch, J. Chem. Phys. 38, 2466 (1963); G. Z. Whitten and B. S. Rabinsvitch, J. Chem. Phys. 41, 1883 (1964); D. C. Tardy, B. S. Rabinovitch, and G. Z. Whitten, J. Chem. Phys. 48, 1427 (1968).